Hopping Conduction in Quasi-1D Titanium Trisulfide Layered Nanoribbons

Abhishek Mishra,[1,2] Ivan A. Verzhbitskiy,[1,2,a)] Rainer Lee,[1,2] Aleksandr Rodin,[3,4] Zhepeng Zhang,[5] Sarthak Das,[1,2] Chit Siong Lau,[1,2,6] Ding Huang,[1,2] Goki Eda,[5,7,8] and Kuan Eng Johnson Goh[1,2,5,9,10,b)]
[1)] *Quantum Innovation Centre (Q. InC), Agency for Science Technology and Research (A*STAR), 2 Fusionopolis Way, Innovis #08-03, Singapore 138634, Republic of Singapore*
[2)] *Institute of Materials Research and Engineering (IMRE), Agency for Science, Technology and Research (A*STAR), 2 Fusionopolis Way, Innovis #08-03, Singapore 138634, Republic of Singapore*
[3)] *Yale-NUS College, 16 College Avenue West, 138527, Singapore*
[4)] *Department of Materials Science and Engineering, National University of Singapore, 117575, Singapore*
[5)] *Department of Physics, National University of Singapore, 2 Science Drive 3, Singapore 117551, Singapore*
[6)] *Science, Mathematics and Technology, Singapore University of Technology and Design, 8 Somapah Road, Singapore 487372, Singapore*
[7)] *Centre for Advanced 2D Materials, National University of Singapore, Singapore 117546, Singapore*
[8)] *Department of Chemistry, National University of Singapore, Singapore 117543, Singapore*
[9)] *Division of Physics and Applied Physics, School of Physical and Mathematical Sciences, Nanyang Technological University, 21 Nanyang Link, Singapore 637371, Singapore*
[10)] *Centre for Quantum Technologies, National University of Singapore, 3 Science Drive 2, Singapore 117543*

(Dated: 13 August 2025)

Quasi-one-dimensional (quasi-1D) layered nanoribbons (NRs) are being extensively investigated for their potential applications in next-generation nanoelectronics and optoelectronics. Understanding electrical conduction in such NRs is essential for designing the devices. In this work, we provide insights into hopping conduction mechanisms in NR transistors based on titanium trisulfide (TiS_3), a quasi-1D layered semiconductor with distinctive anisotropic properties. We report both linear and nonlinear current–voltage characteristics over a temperature range of 5 K - 300 K. The thermal evolution of the nonlinear characteristics exhibits power-law scaling and collapses onto a single universal curve when scaled by temperature. Our findings suggest that the nonlinear conduction is dominated by rare-chain hopping, having its origins in the disorders in TiS_3.

One-dimensional (1D) atomic wires, in principle, offer geometrically confined, anisotropic conduction and excellent electrostatic control over charge carriers, making them ideal channel materials for ultra-scaled nanoelectronic and quantum devices[1]. Prominent examples of quasi-1D materials include carbon nanotubes[2], graphene nanoribbons[3], and transition metal trichalcogenide (TMTC) nanoribbons (e.g., TiS_3, $ZrSe_3$, $TaSe_3$)[4], among others. Low-temperature electrical conduction in these systems has been described by various mechanisms, including, but not limited to, tunneling into Luttinger liquid[5], transport through a Wigner crystal[6], and ballistic conduction[7,8]. However, charge transport in these materials is often obscured by disorders, which are inevitably introduced during material growth and device fabrication[9–12]. In a disordered system, conduction is primarily governed by carrier hopping, as described by the variable-range hopping (VRH) model[13,14]. In effect, carriers hop along paths of least resistance, consisting of energetically favorable and spatially accessible localized states. Presumably, two- and three-dimensional conductors exhibit multiple hopping paths, allowing carriers to bypass regions of higher resistance. In quasi-1D conductors, however, the density of available hopping paths can be severely curtailed[15], strongly affecting charge transport efficiency. It has been shown that hopping in quasi-1D materials can deviate from the conventional VRH model, highlighting the need to reassess hopping mechanisms in low-dimensional systems. In disordered quasi-1D systems with a greatly reduced density of hopping sites, charge conduction occurs via the rare-chain hopping (RCH) mechanism[15,16], particularly at low temperatures. For a comprehensive understanding of electrical conduction in quasi-1D nanoribbons (NRs), it is therefore imperative to explore the conduction in moderately disordered materials and evaluate the hopping mechanism in reduced dimensions. In this work, we explore hopping conduction in quasi-1D layered NRs, such as titanium trisulfide (TiS_3)[17,18], a semiconductor from TMTC family of materials. The structural building blocks of TiS_3 are 1D atomic chains, consisting of one titanium atom and six sulfur atoms arranged in a prism structure. A true-1D material is devoid of inter-chain covalent bonding. However, in low-symmetry materials like TiS_3, the 1D atomic chains are weakly interacting within the single layer, forming a quasi-1D system. These layers are stacked into three-dimensional whiskers by van der Waals (vdW) forces. The inter-layer transport in stacks, however, is largely suppressed due to the van der Waals gap, a hallmark of the transport

[a)] Electronic mail: ivan_verzhbitskiy@imre.a-star.edu.sg
[b)] Electronic mail: kejgoh@yahoo.com

in vdW materials[19]. TiS_3 exhibits gate-tunable conductivity, high theoretically predicted mobility (>10^4 cm^2/Vs)[20], and pronounced anisotropic properties, making it a promising candidate for next-generation nanoelectronic applications. Various conduction mechanisms, including thermally activated transport[21,22] and sliding charge density waves[18,23–25], have previously been proposed to contribute to transport in TiS_3 NRs. However, the impact of disorder on charge transport and the underlying conduction mechanisms in these NRs remain largely unexplored[26,27]. Here, we show that charge conduction in disordered TiS_3 NRs is governed by hopping mechanisms. We examine the linear and nonlinear current–voltage characteristics of TiS_3 over a temperature range from 5 K to 300 K, scrutinizing the potential contributions of various charge transport mechanisms. The electrical conduction in disordered TiS_3 NRs is found to be consistent with the RCH model – a mechanism theoretically predicted for hopping conduction in quasi-1D material systems. Experimentally, RCH conduction has been observed in localized trivial edge states of InAs/GaSb quantum wells[28], metal/amorphous silicon/metal tunnel junctions[29], and Nb_2PdS_5 nanowires[30]. The devices used in this work are back-gated field-effect transistors (FETs) made with TiS_3 NRs, exfoliated from chemical vapor transport (CVT)-grown TiS_3 whiskers. A scanning-electron microscopy (SEM) image of a typical TiS_3 device is shown in Figure 1(a) (Representative Raman spectra of the TiS_3 NRs are shown in Figure S1 of the Supplementary Information). To avoid the impact of Schottky barrier at the contact junctions, we employed ohmic In/Au (5 nm/50 nm) contacts that exhibit temperature-independent low contact resistance for *n*-type conduction in TiS_3 NRs[31]. The 4-wire current-voltage characteristics of three TiS_3 NR FETs, henceforth referred as devices *D1*, *D2* and *D3*, are shown in Figure 1(b-d). As the temperature is lowered from 200 K to 8 K, the current-voltage characteristics of the device *D1* become increasingly nonlinear. On the contrary, the device *D3* retains its linearity in the entire temperature range. While linear through most of the temperature range, characteristics of the device *D2* exhibit small nonlinearity below 50 K, which is highlighted in the upper panel of Figure 2(b). The 2-wire transfer characteristics in the insets of Figures 1(b-d) reveal the gate efficiency of the TiS_3 FETs. Importantly, all three NRs are of similar widths and thicknesses (Figure 1(b-d)), thus reducing the impact of geometrical differences in the following analysis. To highlight the current-voltage nonlinearity in device *D1*, we plot the data in the logarithmic scale (Figure 2(a)). Using the power-law relation ($I \propto V^{\beta}$), we extract the exponent β and summarize its thermal evolution in comparison with devices *D2* and *D3* in the upper panel of Figure 2(b). The clear upturn of the exponent β below 200 K in the device *D1* underlines the strong deviation from linear transport ($\beta = 1$). Moreover, the current and voltage characteristics of device *D1*, when scaled by $T^{\alpha+1}$ and T, respectively, collapse onto the 'universal' curve (Figure 2c) given by the following equation:

$$I = I_0 T^{\alpha+1} \sinh\left(\frac{\gamma V}{2T}\right) |\Gamma\left(1+\frac{\beta}{2}+i\frac{\gamma V}{2\pi T}\right)|^2 \qquad (1)$$

Here, I_0 and γ are fitting parameters, α is the power-law exponent of conductance - temperature characteristics (Figure 2d) and β is the power-law exponent of the current - voltage characteristics (Figure 2a). The equation 1 is generally used to empirically model the electrical conduction in the systems exhibiting nonlinear (power-law) transport[32]. This equation has earlier been used to model tunneling into 1D Luttinger liquid[5] and nonlinear hopping conduction in 1D systems[16]. The collapse of the experimental data onto the universal curve thus corroborates the intrinsic power-law behavior in the current–voltage characteristics of the device *D1*.

We now explore the mechanisms driving the observations discussed above. The power-law behavior in the device *D1* precludes the role of Schottky or Poole-Frenkel emission, which follow non-power-law models. Moreover, the characteristics shown in Figure 1(b-d) were extracted with a 4-wire configuration, indicating the dominant role of the channel, instead of contacts, in imparting the nonlinear behavior. The power-law relation also precludes the formation of pinned Wigner solid phase, which shows nonlinear current-voltage characteristics and $e^{1/T}$ dependence of resistance on temperature (T)[33]. On the other hand, the current-voltage power-law relation is observed when the injected carrier density exceeds the equilibrium carrier density in the channel, leading to the space-charge limited conduction (SCLC). Following this model, the exponent (β) is expected to always be more than or equal to 2 ($\beta \geq 2$)[34]. Here, however, exponents in the range of $1 < \beta < 2$ are also observed, particularly at temperatures higher than 75 K. Therefore, we rule out the role of SCLC in establishing nonlinear conduction in our samples. In a quasi-1D material, the tunneling of an electron into Luttinger liquid may also result in a power-law dependence of conductance and current on temperature and voltage, respectively[5]. In fact, the equation 1 is generally used to model the transport in Luttinger liquid systems. However, unlike the constant value of exponent in the Luttinger Liquid model[35], the exponent β of the device *D1* increases at lower temperatures. Moreover, the formation of the Luttinger liquid requires an extremely clean 1D channel. The inconsistent current-voltage characteristics in devices with similar dimensions (Figure 1), however, suggest the presence of disorder, precluding the observation of the Luttinger liquid behavior in our devices. Indeed, in the absence of a clear correlation between the charge transport characteristics and device dimensions, we attribute the observation of nonlinearity to disorders in the TiS_3 channel. The presence of disorder in the channel is also evident from the device-to-device variations in transfer characteristics shown in the inset of Figures 1(b-d). In the back-gated configuration, field-effect transfer curves show vastly different values of threshold voltages, indicating the variation of the intrinsic charge densities in our devices. Moreover, we note that the threshold voltages of the devices *D1* and *D2* are higher than the threshold voltage of the device *D3* (See transfer characteristics in Figure 1 for threshold voltages). While the exact reason behind this variation is unclear, we emphasize that chalcogen vacancies and other atomistic defects may act as charge donors in TiS_3, altering the intrinsic doping levels[22]. The high threshold voltages of the devices *D1* and *D2* thus indicate relatively higher levels of defect-induced doping in these devices.

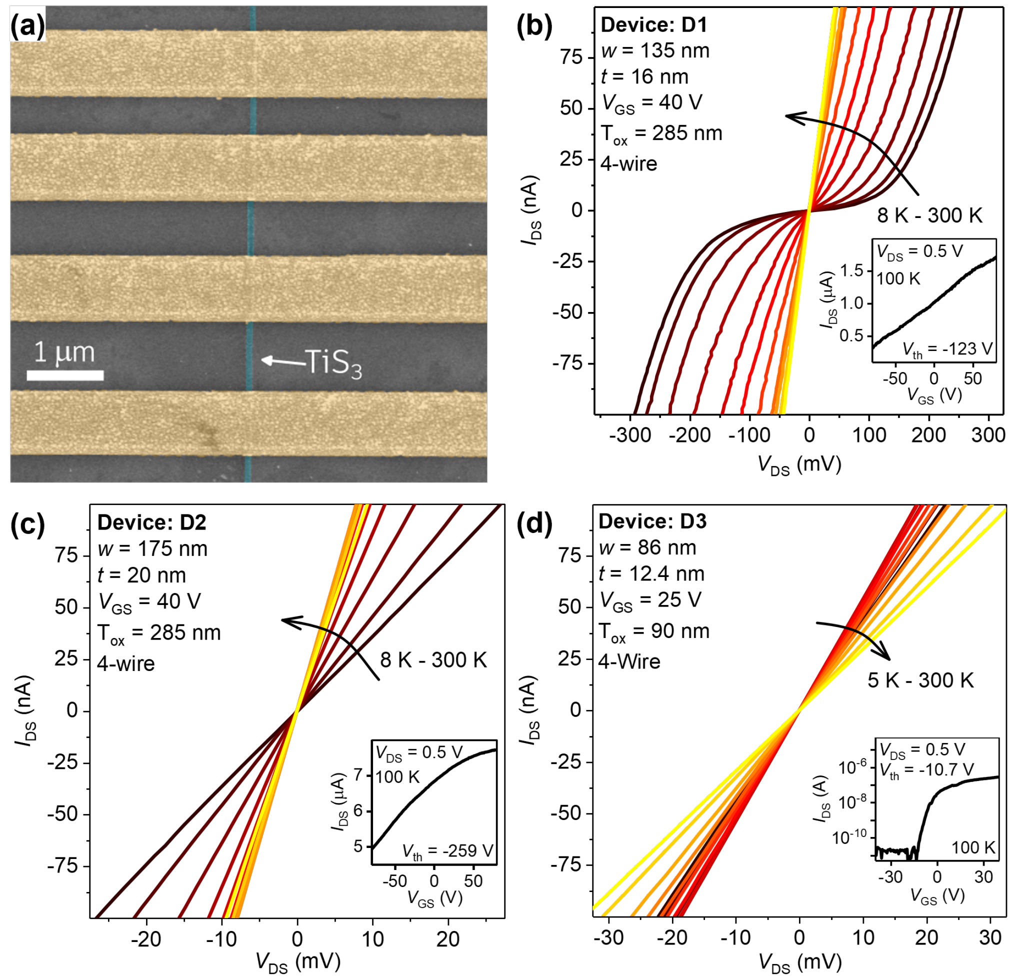

FIG. 1. (a) SEM image of a typical back-gated TiS_3 NR field-effect transistor (FET). (b-d) Current-voltage characteristics of three different TiS_3 NR FETs. The measurements were performed in a 4-wire configuration by sweeping the drain current (I_{DS}) from -100 nA to 100 nA, at a fixed gate voltage (V_{GS}), corresponding to the linear region of operation. The transfer characteristics of the transistors are shown in the inset. The channel length (l) of all devices is ~600 nm. The values of NR's width (w) and thickness (t) are reported in the figure.

The presence of disorder in low-dimensional materials generally results in hopping-based transport[13,14]. Compared with two-dimensional (2D) and three-dimensional (3D) materials, the electrical conduction in quasi-1D materials is extremely prone to disorders[15,36], mandating their consideration in analyzing the conduction through TiS_3 NRs. The hopping-based conduction is often observed in disordered materials, where charge transport happens primarily through hopping in a defect band. The hopping in quasi-1D materials imparts both linear and power-law-related nonlinear features to current-voltage characteristics. The nonlinear features have earlier been explained using the RCH model, which is based on hopping along the chains of highly conductive sites[15,16,36]. The model predicts a power-law relation ($G \propto T^{\alpha}$) between ohmic conductance (G) and temperature (T) in a limited range of temperature. A power-law relation ($I \propto V^{\beta}$) between current (I) and voltage (V) is also observed at high voltages, where β scales with $T^{-1/2}$ (Ref[16]). As shown in Figure 2, the device *D1* exhibits several features consistent with the RCH model.

We note that the ohmic conductance (G) of the device *D1* shows a power-law relation with temperature ($G \propto T^{\alpha}$) with exponent $\alpha \approx 2.58$ in a 70 K $\leq$ T $\leq$ 110 K temperature range (Figure 2(d)). In addition, the current-voltage power-law exponent β (Figure 2(a)) scales linearly with $T^{-1/2}$ (lower panel of Figure 2(b)). These observations indicate the occurrence of RCH conduction in the device *D1*, imparting nonlinearity to its current-voltage characteristics.

Contrary to the power-law characteristics of the device *D1*, the devices *D2* and *D3* (as well as devices *D4* and *D5* presented in Section II of the Supplementary Information) exhibit linear current-voltage characteristics (Figures 1(c,d) and S2), which we attribute to conventional VRH conduction. Following the VRH model, we fit the ohmic conductance of the devices *D2*-*D5* to the following equation[12]:

$$G = G_0(T)exp\left[-\left(\frac{T_0}{T}\right)^{1/(d+1)}\right] \quad (2)$$

Here, T_0 is the characteristic temperature, d is the chan-

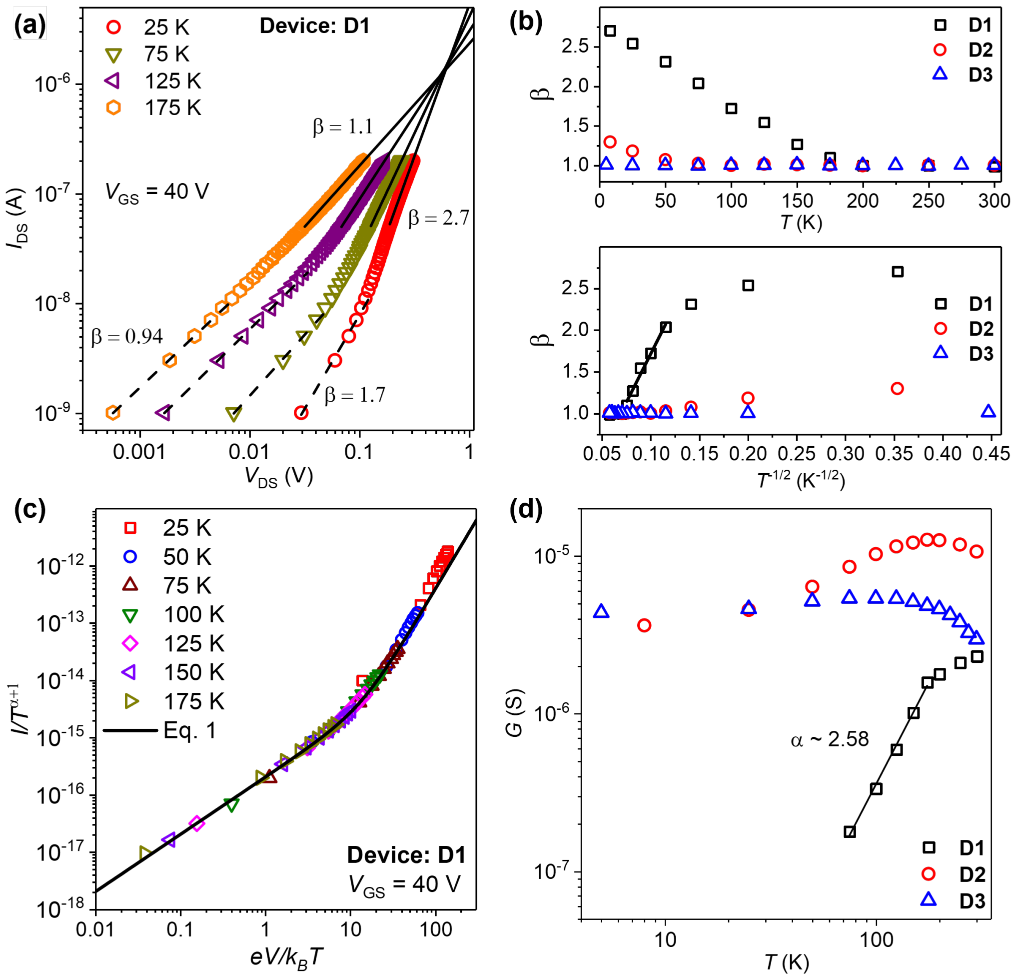

FIG. 2. (a) Current-voltage characteristics of device *D1* plotted on logarithmic scale. The exponent (β) was extracted by two-segment linear fits in low-current and high-current regions, shown as dashed and solid lines, respectively. (b) [Upper Panel] Temperature dependence of the exponent β for the devices shown in Figure 1. [Lower Panel] $\beta - T^{-1/2}$ relation for devices *D1-D3*. (c) The collapse of temperature-dependent current-voltage characteristics onto the universal curve, Equation 1. (d) Ohmic-conductance-temperature characteristics plotted on logarithmic scale. The power-law relation for the device *D1* is highlighted as a linear fit in the region of most robust fit (70 K – 110 K) with exponent $\alpha \approx 2.58$.

nel dimensionality, and $G_0(T) = AT^{-m}$ ($m \sim 0.8 - 1$) is the temperature-dependent pre-factor. The results of the fitting to the 2D VRH model ($d = 2$ in Equation 2) for the devices *D2-D5* are shown in Figure 3 (fittings with slightly higher errors were achieved for $d = 1, 3$, see Section III in Supplementary Information). Notably, using a temperature-independent pre-factor (G_0 in Equation 2; see Section IV in the Supplementary Information) results in poorer fit convergence, indicating a significant role of electron-phonon coupling and inelastic hopping processes[37]. The conductance was also fitted to the model for hopping in presence of anisotropically screened coulomb potential, which follows $lnG \propto T^{-2/5}$ model[38]. The errors from fitting to this particular model were similar to the errors from fitting to the VRH model shown in figure 3 (see section VI in Supplementary Information).

The fittings to the VRH model shown in Figure 3 highlight device-to-device variations and deviations at low temperatures. The variations indicate the presence of mesoscopic fluctuations, typically more important in 1D systems, highlighting the underlying quasi-1D structure. Nevertheless, the stretched-exponential dependence of conductance on temperature (Figure 3) demonstrates that the conductivity in devices *D2-D5* follows the VRH model over limited, sample-dependent temperature ranges. At low temperature, however, the change in conductivity slope indicates the presence of effects likely related to the electronic properties of the material. Although there are a number of different mechanisms that can lead to such deviations, an important one is the variation of the density of hopping states. In VRH model, the characteristic temperature (T_0) depends on the density of states $g : T_0 \sim 1/g$. Assuming the density of states is not constant, T_0 can be interpreted as an effective average over the energy states accessible at a given temperature, resulting in a temperature-dependent T_0. This translates into the temperature-dependent slope of the logarithmic conductivity plot. Although the precise thermal evolution of the effective density of states in our devices remains unknown, analytical studies of conductivity in 1D systems highlight the temperature-dependent nature of T_0 (Ref[39]). Notably, the low temperature deviation from the slope shown by the device *D2* is also accompanied by an onset of nonlinearity at temperatures below 50 K (upper panel in Figure 2(b)), suggesting the transition to RCH conduction. This transition can thus be understood as a progressive evolution of the density of states, limited by the number of energetically accessible hopping sites at lower temperatures, imposing strong, voltage-driven nonlinearities. Interestingly, the ohmic conductivity of the device *D1* can also be fitted to Equation 2, albeit with a higher degree of error (see section V in the Supplementary Information). However, the conventional VRH model alone cannot explain its nonlinear characteristics, suggesting the RCH to be the dominant conduction mechanism at low temperatures.

Having discussed two different hopping conduction models in TiS_3 channel, it is important to highlight their distinguishing features. Phenomenologically, the VRH model describes electrons hopping between spatially separated localized states, with the hopping path determined by energy considerations rather than physical proximity regardless of the dimensionality[14]. The VRH conduction shows stretched-exponential relation between conductance and temperature[14], and ohmic or non-power-law-related[40] current - voltage characteristics. In RCH, on the other hand, the conduction is governed by tunneling along the 1D chains of highly-conductive sites[29]. Driven by RCH, the current-voltage and conductance-temperature characteristics experience distinct power-law dependence[16,29]. Interestingly, the power-law-related characteristics are signatures of various intrinsic transport mechanisms in quasi-1D systems. The power-law-related current-voltage and conductance-temperature characteristics have earlier been observed in electrical measurements of various 1D and quasi-1D material systems, including carbon nanotubes[5], molybdenum selenide[35], niobium triselenide[41,42], tantalum trisulfide[41], indium antimonide[43], among others. However, the presence of defects in the material can suppress the intrinsic transport mechanism, resulting in defect-dominated transport. For example, power-law[41] and stretched-exponentially-related[44] resistance-temperature characteristics have earlier been observed in different samples of niobium triselenide, highlighting the dominance of 1D and defect-dominated hopping transport, respectively, in the same material system. In the special case of rare-chain hopping, the hopping conductance deviates from stretched-exponential dependence on temperature, and follows power-law behavior, shown by the device *D1* here and also in Nb_2PdS_5 NRs reported earlier[30]. It is emphasized that the characteristics of RCH and 1D transport are seemingly similar. A comprehensive understanding of transport in quasi-1D materials, therefore, requires a scrutiny of multiple devices and consideration of disorders.

Our findings suggest that low-temperature conduction in these devices is primarily governed by carrier hopping through localized states. These states arise from defects and disorder that are inevitably introduced during material growth and device fabrication. For instance, sulfur vacancies in TiS_3 exhibit low activation energies and are known to induce significant charge doping[22], even after annealing at temperatures as low as 300 °C in vacuum[17]. Additionally, two distinct TiS_3 morphologies, 2D and quasi-1D, can be obtained by varying the growth temperature between 400 °C and 500 °C (Ref[17]), highlighting the intricate relation between electrical properties, structural characteristics, and defect density. Moreover, thermal oxidation of TiS_3 into TiO_2 (Ref[45,46]) may further contribute to local changes in the channel's band structure. Together, these observations reveal the low structural stability and extreme sensitivity of TiS_3 NRs to atomistic defects, shaping the hopping conduction mechanisms observed in our devices.

In summary, we explored the electrical conduction mechanisms in TiS_3 NR-based transistors. Measurements conducted over a temperature range of 5 K - 300 K revealed two hopping conduction mechanisms, distinguished by the degree of nonlinearity in the current–voltage characteristics and the thermal evolution of conductivity. We observed conventional VRH in NRs exhibiting linear current–voltage behavior, while strong nonlinearities, particularly at low temperatures, were attributed to RCH in the quasi-1D channel. Our results suggest that disorder-driven mechanisms, such as hopping, dominate charge transport in disordered quasi-1D TiS_3 NRs, especially at cryogenic temperatures. Therefore, strategies for precise control of defects will be critical for advancing device applications based on quasi-1D NRs.

SUPPLEMENTARY MATERIAL

The supplementary material contains following additional information: Raman spectra of TiS_3 nanoribbons, current - voltage characteristics of the devices *D4* and *D5*, and results of fitting of conductance of the devices to modified VRH models (considering different values of the exponents and the prefactor).

ACKNOWLEDGMENTS

This research was supported by the Agency for Science, Technology, and Research (A*STAR) (#21709, C230917006, C230917007). I.A.V. and K.E.J.G. acknowledge support from a Singapore National Research Foundation Grant (CRP21-2018-0001). C.S.L. acknowledges support from A*STAR MTC YIRG grant No. M21K3c0124 and MTC IRG grant No. M23M6c0103. D.H. acknowledges funding support from A*STAR Project C222812022 and MTC YIRG M22K3c0105. G.E. acknowledges support from the Ministry of Education (MOE), Singapore, under AcRF Tier 3 (MOE2018-T3-1-005) and Tier 1 (A-8001995-00-00). S.D. acknowledges funding support from A*STAR project C243512017. K.E.J.G. acknowledges support from the National Research Foundation, Singapore through the National Quantum Office, hosted in A*STAR, under its Centre for Quantum Technologies Funding Initiative (S24Q2d0009)

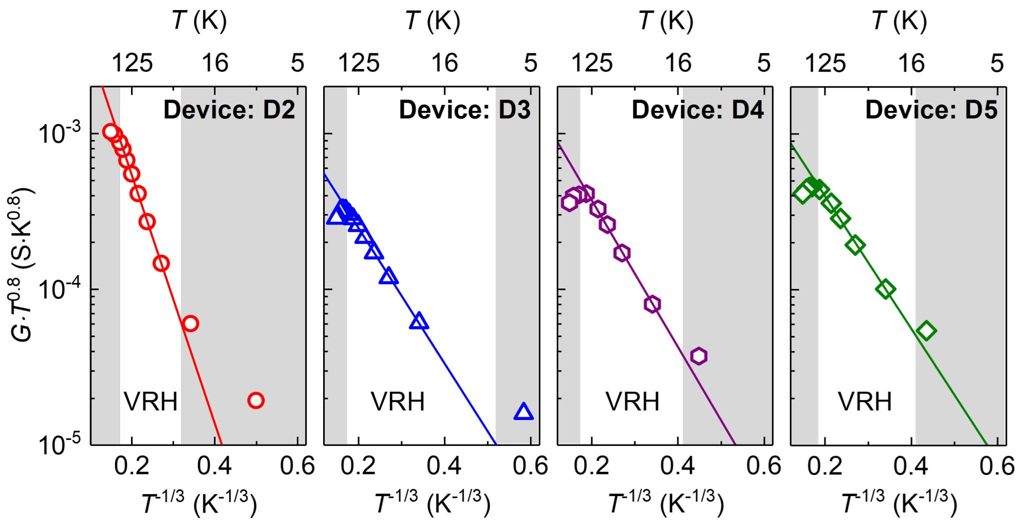

FIG. 3. VRH conduction in the devices *D2 - D5*. The solid line is the fit to Eq. 2. The shaded region indicates the deviations from the VRH model. The top and bottom *x*-axes are in linear scale, while the *y*-axes are in log scale.

DATA AVAILABILITY STATEMENT

The data that support the findings of this study are available from the corresponding author upon reasonable request.

AUTHOR DECLARATIONS

The authors have no conflicts to disclose.

[1] Jia, C.; Lin, Z.; Huang, Y.; Duan, X. Nanowire Electronics: From Nanoscale to Macroscale. Chemical Reviews **2019**, 119, 9074–9135.
[2] Franklin, A. D.; Hersam, M. C.; Wong, H.-S. P. Carbon nanotube transistors: Making electronics from molecules. Science **2022**, 378, 726–732.
[3] Wang, H.; Wang, H. S.; Ma, C.; Chen, L.; Jiang, C.; Chen, C.; Xie, X.; Li, A.-P.; Wang, X. Graphene nanoribbons for quantum electronics. Nature Reviews Physics **2021**, 3, 791–802.
[4] Island, J. O.; Molina-Mendoza, A. J.; Barawi, M.; Flores, R. B. E.; Clamagirand, J. M.; Ares, J. R.; Sánchez, C.; van der Zant, H. S.; DÁgosta, R.; Ferrer, I. J.; Castellanos-Gomez, A. Electronics and optoelectronics of quasi-1D layered transition metaltrichalcogenides. 2D Materials **2017**, 4, 022003.
[5] Bockrath, M.; Cobden, D. H.; Lu, J.; Rinzler, A. G.; Smalley, R. E.; Balents, L.; McEuen, P. L. Luttinger-liquid behaviour in carbon nanotubes. Nature **1999**, 397, 598–601.
[6] Deshpande, V. V.; Bockrath, M. The one-dimensional Wigner crystal in carbon nanotubes. Nature Physics **2008**, 4, 314–318.
[7] Javey, A.; Guo, J.; Wang, Q.; Lundstrom, M.; Dai, H. Ballistic carbon nanotube field-effect transistors. nature **2003**, 424, 654–657.
[8] Baringhaus, J.; Ruan, M.; Edler, F.; Tejeda, A.; Sicot, M.; Taleb-Ibrahimi, A.; Li, A.-P.; Jiang, Z.; Conrad, E. H.; Berger, C.; Tegenkamp, C.; de Heer, W. A. Exceptional ballistic transport in epitaxial graphene nanoribbons. Nature **2014**, 506, 349–354.
[9] Mukherjee, S. et al. Toward Phonon-Limited Transport in Two-Dimensional Transition Metal Dichalcogenides by Oxygen-Free Fabrication. ACS Nano **2025**, 19, 9327–9339, PMID: 39993723.
[10] Chowdhury, T.; Sadler, E. C.; Kempa, T. J. Progress and Prospects in Transition-Metal Dichalcogenide Research Beyond 2D. Chemical Reviews **2020**, 120, 12563–12591.
[11] Chen, Z.; Narita, A.; Müllen, K. Graphene nanoribbons: on-surface synthesis and integration into electronic devices. Advanced Materials **2020**, 32, 2001893.
[12] Hsieh, K.; Kochat, V.; Zhang, X.; Gong, Y.; Tiwary, C. S.; Ajayan, P. M.; Ghosh, A. Effect of Carrier Localization on Electrical Transport and Noise at Individual Grain Boundaries in Monolayer MoS2. Nano Letters **2017**, 17, 5452–5457, PMID: 28786685.
[13] Ambegaokar, V.; Halperin, B. I.; Langer, J. S. Hopping Conductivity in Disordered Systems. Phys. Rev. B **1971**, 4, 2612–2620.
[14] Shklovskii, B.; Luryi, S.; Efros, A. Electronic Properties of Doped Semiconductors; Springer Series in Solid-State Sciences; Springer Berlin Heidelberg, 2013.
[15] Rodin, A. S.; Fogler, M. M. Hopping transport in systems of finite thickness or length. Phys. Rev. B **2011**, 84, 125447.
[16] Rodin, A. S.; Fogler, M. M. Apparent Power-Law Behavior of Conductance in Disordered Quasi-One-Dimensional Systems. Phys. Rev. Lett. **2010**, 105, 106801.
[17] Island, J. O.; Barawi, M.; Biele, R.; Almazán, A.; Clamagirand, J. M.; Ares, J. R.; Sánchez, C.; van der Zant, H. S. J.; Álvarez, J. V.; DÁgosta, R.; Ferrer, I. J.; Castellanos-Gomez, A. TiS3 Transistors with Tailored Morphology and Electrical Properties. Advanced Materials **2015**, 27, 2595–2601.
[18] Randle, M. et al. Gate-Controlled Metal-Insulator Transition in TiS3 Nanowire Field-Effect Transistors. ACS Nano **2019**, 13, 803–811.
[19] Das, S.; Appenzeller, J. Where Does the Current Flow in Two-Dimensional Layered Systems? Nano Letters **2013**, 13, 3396–3402, PMID: 23802773.
[20] Dai, J.; Zeng, X. C. Titanium Trisulfide Monolayer: Theoretical Prediction of a New Direct-Gap Semiconductor with High and Anisotropic Carrier Mobility. Angewandte Chemie International Edition **2015**, 54, 7572–7576.
[21] Finkman, E.; Fisher, B. Electrical transport measurements in TiS3. Solid State Communications **1984**, 50, 25–28.
[22] Sun, M.; Li, J.; Ji, Q.; Lin, Y.; Wang, J.; Su, C.; Chiu, M.-H.; Sun, Y.; Si, H.; Palacios, T.; Lu, J.; Xie, D.; Kong, J. Anomalous heavy doping in chemical-vapor-deposited titanium trisulfide nanostructures. Phys. Rev. Mater. **2021**, 5, 094002.
[23] Huang, C.; Zhang, E.; Yuan, X.; Wang, W.; Liu, Y.; ChengZhang; Ling, J.; Liu, S.; Xiu, F. Tunable charge density wave in TiS3 nanoribbons*. Chinese Physics B **2017**, 26, 067302.
[24] Gorlova, I.; Zybtsev, S.; Pokrovskii, V.; Bolotina, N.; Verin, I.; Titov, A. Nonlinear conductivity of quasi-one-dimensional layered compound TiS3. Physica B: Condensed Matter **2012**, 407, 1707–1710, Proceedings of the International Workshop on Electronic Crystals (ECRYS-2011).
[25] Gorlova, I.; Zybtsev, S.; Pokrovskii, V.; Bolotina, N.; Gavrilkin, S.; Tsvetkov, A. Magnetotransport and power-law I-V curves of the layered quasi one-dimensional compound TiS3. Physica B: Condensed Matter **2015**, 460, 11–15, Special Issue on Electronic Crystals (ECRYS-2014).

[26] Trunkin, I. N.; Gorlova, I. G.; Bolotina, N. B.; Bondarenko, V. I.; Chesnokov, Y. M.; Vasiliev, A. L. Defect structure of TiS3 single crystals with different resistivity. Journal of Materials Science **2021**, 56, 2150–2162.

[27] Hsieh, P.-L.; Jackson, C.; GrÃ¼ner, G. Disorder effects in the linear chain compound TiS3. Solid State Communications **1983**, 46, 505–507.

[28] Sazgari, V.; Sullivan, G.; Kaya, i. d. I. i. d. I. Localization of trivial edge states in InAs/GaSb composite quantum wells. Phys. Rev. B **2019**, 100, 041404.

[29] Xu, Y.; Ephron, D.; Beasley, M. R. Directed inelastic hopping of electrons through metal-insulator-metal tunnel junctions. Phys. Rev. B **1995**, 52, 2843–2859.

[30] Ning, W.; Yu, H.; Wang, N.; Liu, Y.; Han, Y.; Yang, J.; Du, H.; Zhang, C.; Yang, K.; Tian, M.; Zhang, Y. Nonlinear transport in quasi-one-dimensional Nb2PdS5 nanowires. Applied Physics Letters **2014**, 105, 172603.

[31] Verzhbitskiy, I. A.; Mishra, A.; Mitra, S.; Zhang, Z.; Das, S.; Lau, C. S.; Lee, R.; Huang, D.; Eda, G.; Ang, Y. S.; Goh, K. E. J. Low-Temperature Contacts and the Coulomb Blockade Effect in Layered Nanoribbons with In-Plane Anisotropy. ACS Nano **0**, 0, null, PMID: 40081405.

[32] Worne, J. H.; Anthony, J. E.; Natelson, D. Transport in organic semiconductors in large electric fields: From thermal activation to field emission. Applied Physics Letters **2010**, 96, 053308.

[33] Madathil, P. T.; Rosales, K. A. V.; Chung, Y. J.; West, K. W.; Baldwin, K. W.; Pfeiffer, L. N.; Engel, L. W.; Shayegan, M. Moving Crystal Phases of a Quantum Wigner Solid in an Ultra-High-Quality 2D Electron System. Phys. Rev. Lett. **2023**, 131, 236501.

[34] Mark, P.; Helfrich, W. Space-Charge-Limited Currents in Organic Crystals. Journal of Applied Physics **1962**, 33, 205–215.

[35] Venkataraman, L.; Hong, Y. S.; Kim, P. Electron Transport in a Multichannel One-Dimensional Conductor: Molybdenum Selenide Nanowires. Phys. Rev. Lett. **2006**, 96, 076601.

[36] Rodin, A. S.; Fogler, M. M. Numerical studies of variable-range hopping in one-dimensional systems. Phys. Rev. B **2009**, 80, 155435.

[37] Ortuño, M.; Estellés-Duart, F.; Somoza, A. M. Numerical Simulations of Variable-Range Hopping. physica status solidi (b) **2022**, 259, 2100340.

[38] Fogler, M. M.; Teber, S.; Shklovskii, B. I. Variable-range hopping in quasi-one-dimensional electron crystals. Phys. Rev. B **2004**, 69, 035413.

[39] Raikh, M.; I.M., R. Fluctuations of the hopping conductance of one-dimensional systems. Journal of Experimental and Theoretical Physics **1989**, 68, 1113.

[40] Papadopoulos, N.; Steele, G. A.; van der Zant, H. S. J. Efros-Shklovskii variable range hopping and nonlinear transport in $1T/1T'-\mathrm{MoS}_2$. Phys. Rev. B **2017**, 96, 235436.

[41] Zaitsev-Zotov, S. V.; Pokrovskii, V. Y.; Monceau, P. Transition to 1D conduction with decreasing thickness of the crystals of TaS3 and NbSe3 quasi-1D conductors. Journal of Experimental and Theoretical Physics Letters **2001**, 73, 25–27.

[42] Slot, E.; Holst, M. A.; van der Zant, H. S. J.; Zaitsev-Zotov, S. V. One-Dimensional Conduction in Charge-Density-Wave Nanowires. Phys. Rev. Lett. **2004**, 93, 176602.

[43] Zaitsev-Zotov, S. V.; Kumzerov, Y. A.; Firsov, Y. A.; Monceau, P. Luttinger-liquid-like transport in long InSb nanowires. Journal of Physics: Condensed Matter **2000**, 12, L303.

[44] Zaitsev-Zotov, S. Transport properties of TaS3 and NbSe3 crystals of nanometer-scale transverse dimensions. Microelectronic Engineering **2003**, 69, 549–554, Proceedings of the Symposium and Summer School on: Nano and Giga Challenges in Microelectronics Research and Opportunities in Russia.

[45] Iyikanat, F.; Sahin, H.; Senger, R. T.; Peeters, F. M. Vacancy Formation and Oxidation Characteristics of Single Layer TiS3. The Journal of Physical Chemistry C **2015**, 119, 10709–10715.

[46] Qin, J.-K.; Sun, H.-L.; Huang, P.-Y.; Li, Y.; Zhen, C.-Y., Liangand Xu Synaptic plasticity realized by selective oxidation of TiS3 nanosheet forneuromorphic devices. RSC Adv. **2023**, 13, 14849–14854.